Earthq Eng & Eng Vib (2010) 9: 39-50 **DOI**: 10.1007/s11803-009-8131-7

Shake table test of soil-pile groups-bridge structure interaction in liquefiable ground

Tang Liang[1†], Ling Xianzhang[1‡], Xu Pengju[1§], Gao Xia[1†] and Wang Dongsheng[2‡]

1. School of Civil Engineering, Harbin Institute of Technology, Harbin 150090, China
2. Research Centre of Road and Bridge Engineering, Dalian Maritime University, Dalian 116026, China

Abstract: This paper describes a shake table test study on the seismic response of low-cap pile groups and a bridge structure in liquefiable ground. The soil profile, contained in a large-scale laminar shear box, consisted of a horizontally saturated sand layer overlaid with a silty clay layer, with the simulated low-cap pile groups embedded. The container was excited in three El Centro earthquake events of different levels. Test results indicate that excessive pore pressure (EPP) during slight shaking only slightly accumulated, and the accumulation mainly occurred during strong shaking. The EPP was gradually enhanced as the amplitude and duration of the input acceleration increased. The acceleration response of the sand was remarkably influenced by soil liquefaction. As soil liquefaction occurred, the peak sand displacement gradually lagged behind the input acceleration; meanwhile, the sand displacement exhibited an increasing effect on the bending moment of the pile, and acceleration responses of the pile and the sand layer gradually changed from decreasing to increasing in the vertical direction from the bottom to the top. A jump variation of the bending moment on the pile was observed near the soil interface in all three input earthquake events. It is thought that the shake table tests could provide the groundwork for further seismic performance studies of low-cap pile groups used in bridges located on liquefiable groun.

Keywords: liquefiable ground; seismic soil-pile-structure interaction; pile groups of bridge; shake table test

1 Introduction

It is well known that soil liquefaction is one of the main causes of earthquake-induced damage to bridge piles, and the significance of this damage has been clearly demonstrated in many earthquakes, most notably the 1995 Hyogo-ken Nambu Earthquake in Japan, and the 1976 Tangshan Earthquake in China. Although soil liquefaction might reduce the inertial force of the superstructure, damage was often attributed to failure of the piles (Fujii et al., 1998; Finn and Fujita, 2002). Therefore, it is important to consider seismic soil-pile-structure interaction in the design of piles, particularly in liquefiable ground conditions. However, since less attention has been paid to the behavior of this type of pile groups, there is currently only limited information available regarding the seismic response of low-cap pile groups and bridge structures in liquefiable ground (Abdoun and Dobry, 2002; Boulanger *et al.*, 1999). More recently, these types of piles have been widely adopted in bridge engineering, especially for bridges built in soil susceptible to liquefaction. There is not much physical modeling data available to understand the mechanisms of soil-low-cap pile group-bridge structure interaction in liquefied soil, nor are there procedures available for the design of this type of pile group (Ohtsuki *et al.*, 1998; Imamura *et al.*, 2004; Li and Yuan, 2004; Ling *et al.*, 2004).

A shake table test was conducted in 2006 to gain insight into the mechanisms of seismic soil-pile-structure interaction for low-cap pile groups and understand the dynamic behavior of pile groups and the bridge structure in liquefiable ground. Meanwhile, one of the key tasks of this test was to generate reliable data, which could be used to improve analysis techniques and design guidelines for low-cap pile groups. In this paper, the shake table test results are presented and analyzed.

Correspondence to: Tang Liang, School of Civil Engineering, Harbin Institute of Technology, Harbin 150090, China
Tel: 86-451-86127799
E-mail: hit_tl@163.com
†PhD Student; ‡Professor; §Associate Professor

Supported by: Major Research Plan of National Natural Science Foundation of China Under Grant No. 90815009; National Natural Science Foundation of China Under Grant No. 50378031 and 50178027; Western Transport Construction Technology Projects Under Grant No. 2009318000100
Received November 9, 2008; **Accepted** March 29, 2009

2 Desciption of test facilities and conditions

2.1 Test facility

The shake table test was performed at the State Key Laboratory for Disaster Reduction in Civil Engineering, Tongji University, Shanghai, China, using the MTS shake table facility. The table is three-dimensional and has six degrees-of-freedom motion. The dimension of the table is 4 m × 4 m, and the maximum payload is 25, 000 kg. The shake table vibrates with two maximum horizontal

accelerations of 1.2 g and 0.8 g, and a maximum acceleration of 0.7 g vertically. Its frequency ranges from 0.1 to 50 Hz and there are 96 channels available for data acquisition during the testing progress.

2.2 Laminar shear box

A large-scale laminar shear box was designed to study the seismic pile group-soil-bridge structure interaction (Wu *et al.*, 2002). The box is 2 m high, 1.5 m wide and 2 m long (in the major shaking direction); its moving parts weigh approximately 0.7 t. It is typically 5% of the weight of the entire test model including the shear box. The shear box was designed to be sufficiently light when compared to the model. Therefore, the shear box can produce an approximate one-dimensional wave propagation field.

2.3 Test soil

The soil profiles used in the test consisted of two horizontal soil layers. The test sand, with a non-uniformity coefficient of 3.0, mean particle diameter of 0.32 mm, density of 2.72, maximum void ratio of 0.96, minimum void ratio of 0.57 and maximum diameter of 2 mm, was obtained in Shanghai, China. The laminar shear box was partially filled with water in advance, and after that, the unwashed sand was directly placed into it, using a free fall method for the saturated sand layer (Ling *et al.*, 2005), i.e., the sand was lifted to a pre-specified height and dropped into the box through a cone. The dropping height was determined according to the required relative density. Special attention was given so that the sand layer was as homogeneous and loose as possible. The height of the lower sand layer was 1.6 m with an average void ratio of 0.8, relative density of 60% and permeability coefficient of about 0.0035 cm/s. This method for the saturated sand has been used successfully in previous model studies (Ling *et al.*, 2004). The 0.3 m thick upper layer was a normally consolidated reconstituted silty clay for the "model clay". The model clay had liquid and plastic limits of LL45 and PL28, and a plasticity index of PI17. In order to ensure that the sand layer was completely submerged, the water table was approximately at the interface between the upper clay layer and lower saturated sand layer.

2.4 Model structure

A low-cap four-pile group with a single pier was used in the test. The reinforced concrete piles, cap and column pier were modeled with fine-aggregate concrete and galvanized fine iron wires. All the bars embedded in the model structure were replaced by galvanized iron wire with different diameters and had the same bar mark "Φ". The vertical reinforcements, which consisted of 9 Φ2 bars evenly distributed around a circle with a diameter of 70 mm, were embedded in each pile with a diameter of 80 mm. The confinement to the vertical steel was provided by Φ1 bar spirals with a pitch of 20 mm, especially with a pitch of 10 mm within the range of 600 mm of the piles near the cap. A 5 mm concrete cover of the piles was maintained to protect the reinforcement bars. The vertical reinforcement of the 160 mm diameter pier consisted of 32 Φ2 bars evenly distributed around a circle with a diameter of 150 mm, and the confinement to the vertical steel was provided by Φ1 bar spirals with a pitch of 20 mm, especially with a pitch of 10 mm within the range of 150 mm of the pier bottom. A 5 mm concrete cover of the pier was maintained. In addition, the pile groups were lined up 2 by 2 with a spacing of 3.75 times diameter of the pile. Based on the concrete material specimen tests, the fine-aggregate concrete had an average 28-day compressive strength of 8.5 MPa. Considering the fact that simply supported girder bridges have been widely used in bridge engineering, the superstructure in the test was represented by an individual mass of 360 kg on the top of the pier to characterize the inertial effect of the bridge structure.

2.5 Test procedure

To ensure an effective transmission of the table motion to the base of the test ground, the soil container was firmly mounted on the shake table using bolt connections. Detailed construction of the shake table test including the layout of the transducers, the geometry and the pile group system are shown in Fig.1. The model

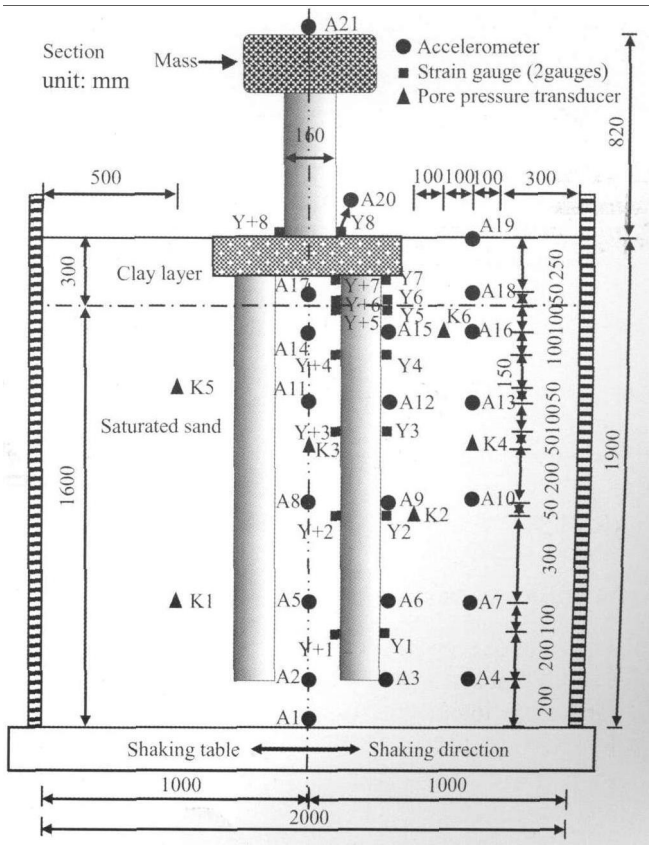

Fig. 1 Schematic figure of the test system

structure was installed into the laminar shear box before the box was filled with test sand. The pile tip was located in the sand at a depth of 1700 mm. The arrangement of the instrumentation, which basically consisted of 8 pairs of strain gauges (Y1 to Y8 and Y1+ to Y8+) attached to the pile and at the pier bottom, 21 accelerometers in the soil and on the pile, and 6 pore pressure transducers in the sand layer, is shown in Fig.1. A pair of strain gauges was fixed on the piles at the same depth. The accelerometers in the soil layer were installed in the perspex boxes, were able to follow the movement of the soil layer simultaneously during shaking. All transducers in the soil were sealed for waterproofing. The effectiveness of this installation method was confirmed in preliminary shake table test studies conducted in 2002.

It was suggested that excessive earthquake shaking conducted before a soil liquefaction test detracts from its successful execution. In order to avoid these disadvantages in the tests, the container base was excited by micro-amplitude white noise and three El Centro earthquake events, summarized in Table 1. The suite of shaking events began with very low-level shaking to characterize the low-strain response of soil and the soil-structure system, and then successively progressed through very strong motions to bring the piles into the nonlinear stage and to cause soil liquefaction. In order to investigate the effect of the frequency component of the input acceleration on soil liquefaction, Event B was scaled by the time scaling factor of $1/\sqrt{10}$ relative to Event C. The dominant frequency of the input acceleration between Event B and Event C was apparently different. Events C and D had a peak amplitude of 0.15 g and 0.5 g, respectively, occurring at the same time. The interval between two shaking events was long enough to dissipate the EPP generated in last event.

Table 1 Suite of shaking events

Event	Motion	Base input, A_{max} (g)
A	White noise	0.002
B	Scaled El Centro earthquake (NS)	0.15
C	El Centro earthquake (NS)	0.15
D	El Centro earthquake (NS)	0.50

3 Test results

3.1 Natural characteristics

Figure 2 shows some pictures of the test model taken after the test set-up. The fundamental frequency and the damping ratio of the test system are about 12.5 Hz and 15.6%, respectively, obtained from the micro-amplitude white noise scanning test performed before the seismic shaking runs. The frequency of the empty box was 1.4 Hz under small-amplitude input acceleration. The empty box was given an initial horizontal displacement of 5 cm and released, and then the frequency and the damping ratio were about 1.2 Hz and 3.53%, respectively. It is obvious that the fundamental frequency and the damping ratio of the empty box were not similar to the test system, so that the dynamic effect of the soil box on the seismic response of the test system would be unremarkable.

3.2 Macroscopic phenomena

The following phenomena were observed from this test. In Event B, where the vibration amplitude of the pier was small while the vibration frequency was relatively high, waterspouts on the ground surface did not occur. In Event C, the vibration amplitude of the superstructure was still very small but the vibration frequency decreased and the top of the sand layer was partly liquefied. In Event D, with 0.5 g input acceleration, significant liquefaction occurred in the sand layer, and sandboils and waterspouts appeared during shaking, as shown in Fig. 2. Many sand hillocks formed by sandboils were distributed on the ground surface, the soil subsidence ranged from 3 to 5 cm, and the settlement of the pile groups ranged from 10 to 17 cm, although the piles did not fail. A number of transverse cracks on the piles, mainly distributed within the pile near the cap were observed, and the pier was still in good condition. The first crack on the piles appeared near the pile heads and some cracks were observed at a soil depth of about 120 cm, which indicated that the inertial force of the superstructure and seismic pile-soil-structure interaction had a significant effect on the seismic performance of the piles in liquefiable ground. It was concluded that the shake table test adequately reproduced the soil liquefaction and the seismic response of the pile groups and the bridge structure in liquefiable ground.

3.3 Liquefaction characteristics of the ground

Time histories of excess pore pressure (EPP) and the EPP ratio are presented in Fig. 3 to Fig. 5 for a variety of depths of the sand profile in events B, C and D. It appears that the EPP gradually increased with soil depth in events B, C and D. This is because the vertical static effective stress in the overlaid soil was greater, regardless of the size of the dynamic shear stress of the lower soil layer. Compared with Event C, the EPP and its ratio were relatively small in Event B, which indicates that the duration of the earthquake seemed to have a noticeable effect on the pore pressure generation. The EPP almost immediately began to dissipate after reaching its peak in events B and C. It can be concluded from these results that EPP was directly impacted by the seismic duration and soil depth. The maximum EPP ratio gradually decreased to a value between 0.2 and 0.3 from the bottom to the top in the vertical direction in Event B, which shows good agreement with the absence of waterspouts on the ground surface. In Event C, the EPP ratio also gradually decreased, but took on values of about 0.4 to 0.5 from the bottom to the top in the

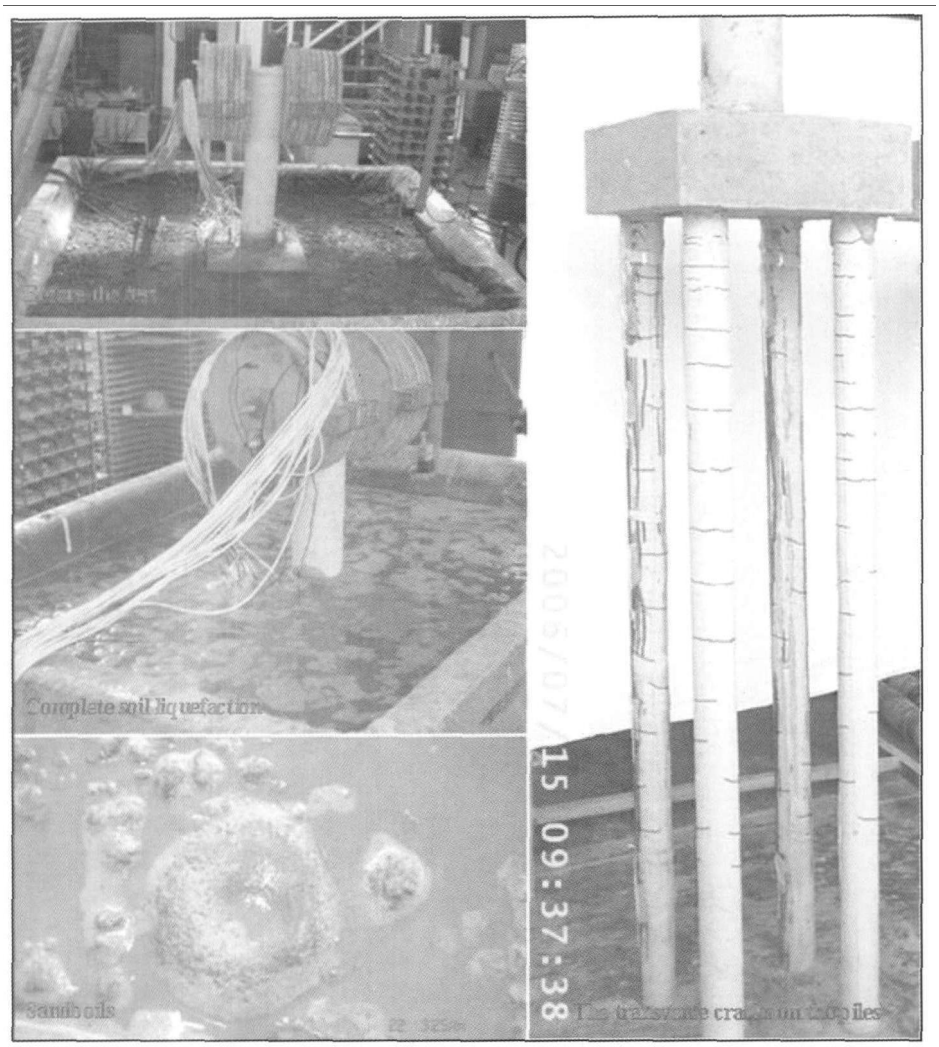

Fig. 2 Test phenomenon

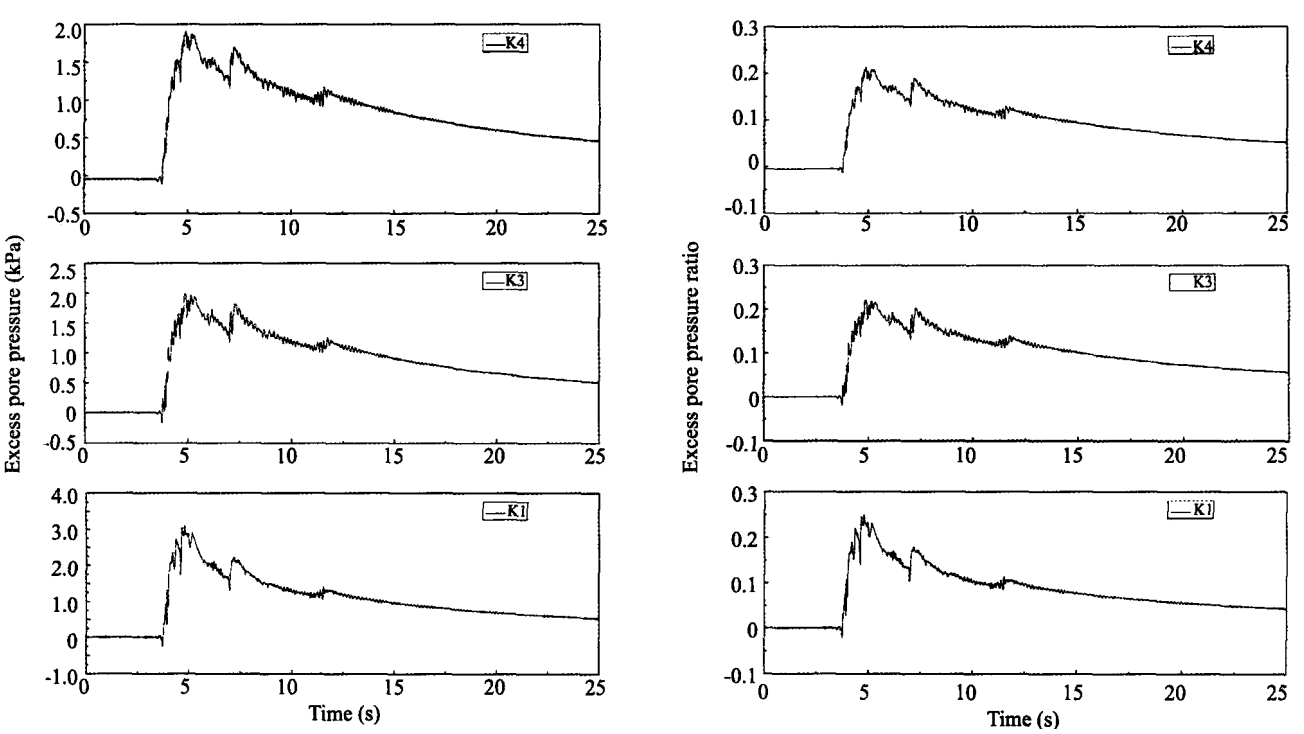

Fig. 3 Time histories of EPP (left) and EPP ratio (right) recorded in Event B

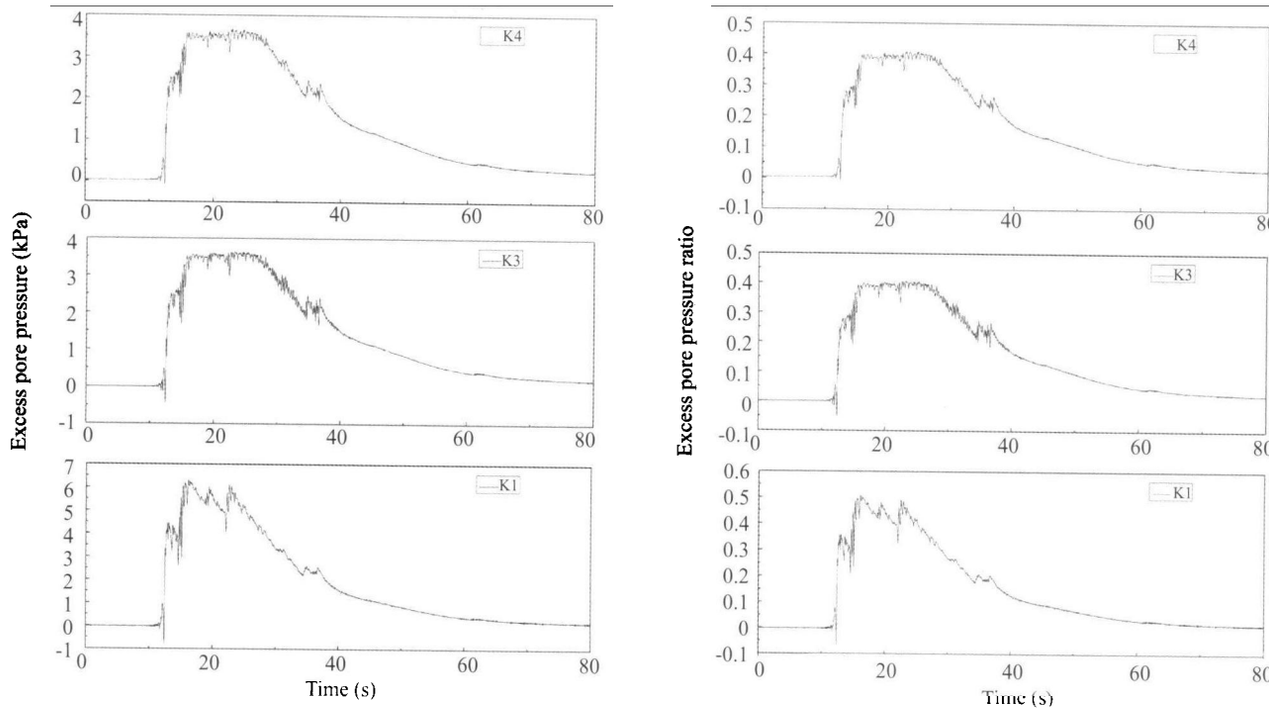

Fig. 4 Time histories of EPP (left) and EPP ratio (right) recorded in Event C

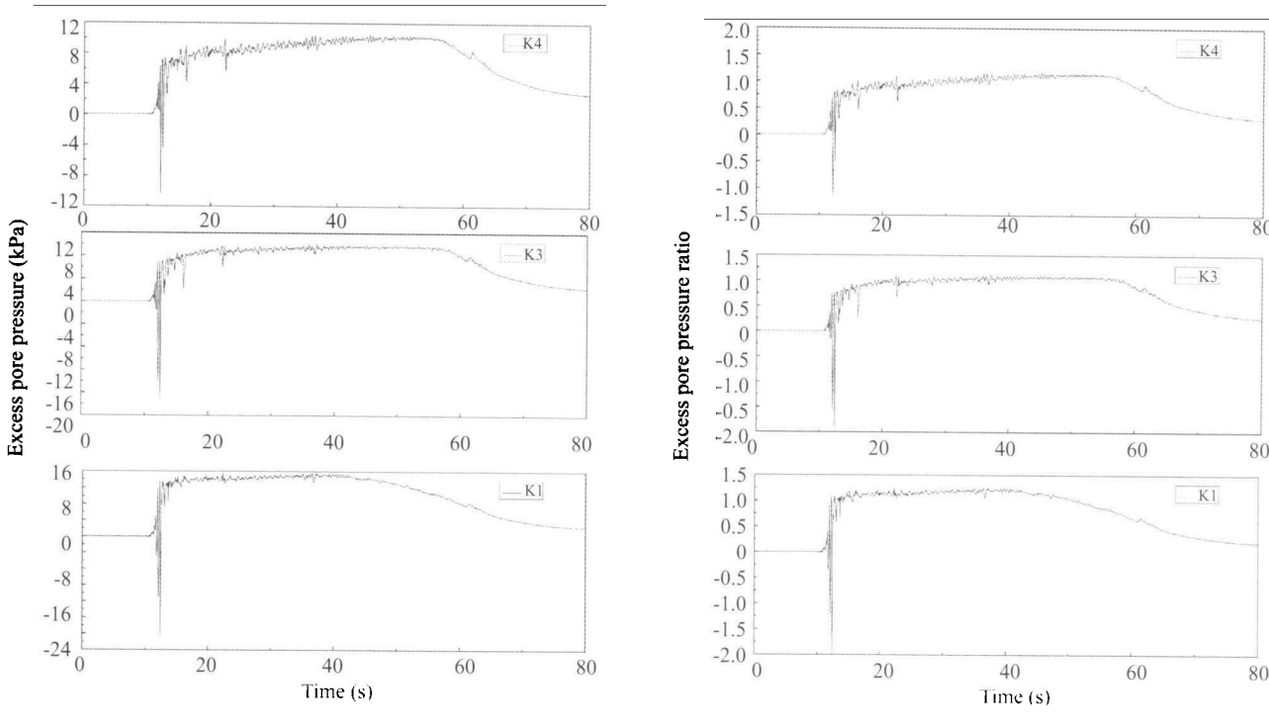

Fig. 5 Time histories of EPP (left) and EPP ratio(right) recorded in Event D

vertical direction. The sand sample in the laboratory testing might exhibit slight soil liquefaction when the EPP ratio ranged between 0.3 and 0.7 (Shi and Wang, 1999). According to the research findings (Shi and Wang, 1999) and the observed phenomena in the test, slight soil liquefaction occurred in the sand in Event C. The EPP ratio rapidly increased and exceeded 1.0 from the bottom to the top in the vertical direction in Event D. After reaching its peak, the EPP maintained its level for the 30 to 50 s duration and did not immediately dissipate, which explains why significant liquefaction in Event D. The time when the EPP ratio quickly increased was near to the time when the input acceleration reached its peak, but the peak EPP ratio exhibited an obvious time lag in different earthquake events, which was more distinct in Event D. The maximum EPP ratio of the sand layer occurred at almost the same time in the same earthquake event. Therefore, the strongest liquefaction

lagged behind the input peak acceleration. Note that more extensive liquefaction occurred and the EPPs showed greater increase and slower dissipation in Event D when compared to Event C, which indicates that the magnitude of the input acceleration has a significant influence on the EPP. The dissipation rate of the EPP in the sand layer from the bottom to the top almost kept a good agreement in events B, C and D. It was also found that the EPP accumulated slowly under small-amplitude shaking in the early stage of events B, C and D, but an obvious accumulation of EPP was observed at the strongest shaking stage in these events.

The instantaneous negative pore pressure was clearly observed near the time when the input acceleration reached its peak in different earthquake events. Note that the maximum absolute value of the negative pore pressure was much larger than the positive peak pore pressure in Event D, which was observed in a former study. Some scholars explained that the positive pore pressure generation was due to the instantaneous shear dilatancy of the sand (Kagawa *et al.*, 1994). That might be caused by the relative movement between the soil and the pore pressure transducers, which instantaneously resulted in a sharp pressure reduction in the cavity of the pore pressure transducers.

Acceleration time histories and the corresponding Fourier spectrum of the sand layer located far from the piles, which can be approximately considered as the free field motion, obtained from the vertical array in events B, C and D are shown in Figs. 6 to 8. As a result of the slight disturbance in the sand, input acceleration attenuation was observed and the acceleration response gradually decreased from the bottom to the top in the vertical direction in Event B. Acceleration response of the sand layer in the free field slightly increased from the bottom to the top in Event C. The EPP developed rapidly and the sand layer quickly liquefied in Event D, which basically destroyed the soil structure. Therefore, the acceleration of the sand layer gradually increased from the bottom to the top as the shear action intensified in the liquefied soil. This comparison illustrates that the acceleration response of the sand layer is highly dependent on the degree of soil liquefaction. In event B, the acceleration response of the sand was dominated by the low-frequency content of the motion and increased in the low-frequency band from the bottom to the top;

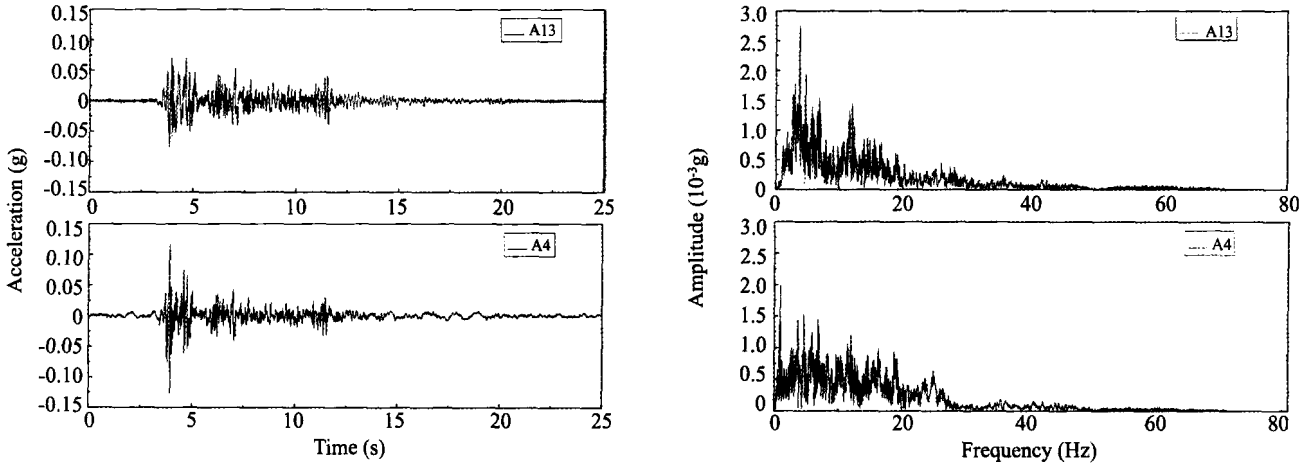

Fig. 6 Acceleration time histories (left) and corresponding Fourier spectra (right) of the ground in the free field in Event B

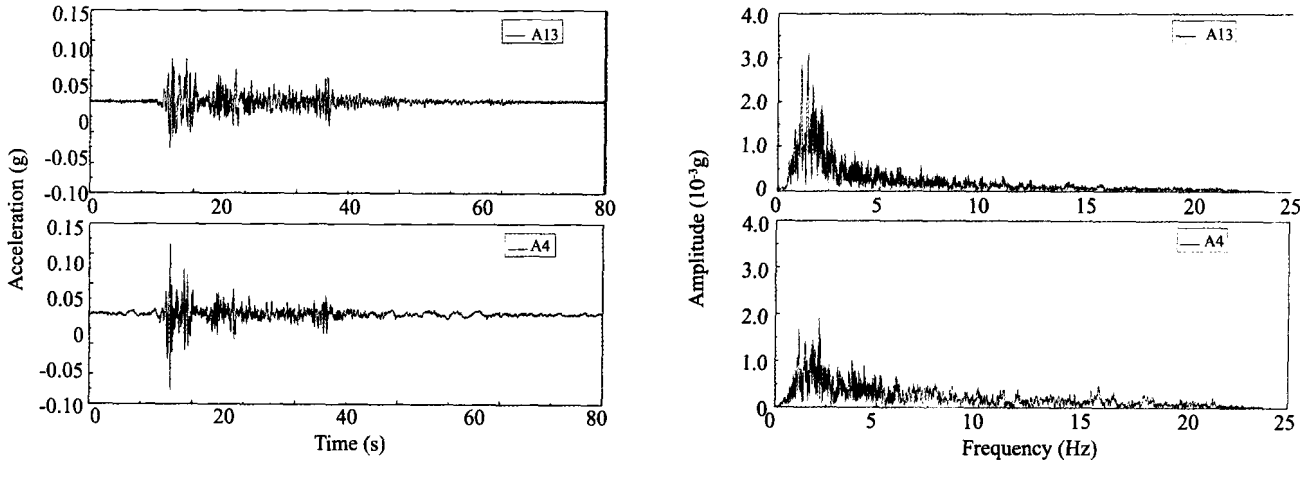

Fig. 7 Acceleration time histories (left) and corresponding Fourier spectra (right) of the ground in the free field in Event C

the middle and high frequency content only slightly changed. However, the motion was seen to be strongly affected as it propagated through the fully liquefied soil layer in Event D. The acceleration response of the sand did not vary in the low-frequency band from the bottom to the top, and the middle and high frequency contents were almost removed when they got through the liquefied soil in Event D. It can be concluded that sand liquefaction has a filter effect on the middle and high frequency contents of the input acceleration.

The displacement time histories of the sand obtained by double-integrating the acceleration measured by accelerometers of the vertical array in the free field are shown in Fig.9. Note that in Event B, the time when the sand displacement reached its peak is nearly the same as the input acceleration. In events C and D, the time when the peak displacement of sand reached its peak lagged behind the input acceleration. Note that the displacement of the fully liquefied sand in the upper sand area retained the higher value for a long time in Event D, which might have been caused by the intensive come-and-go shear flow action of the liquefied sand.

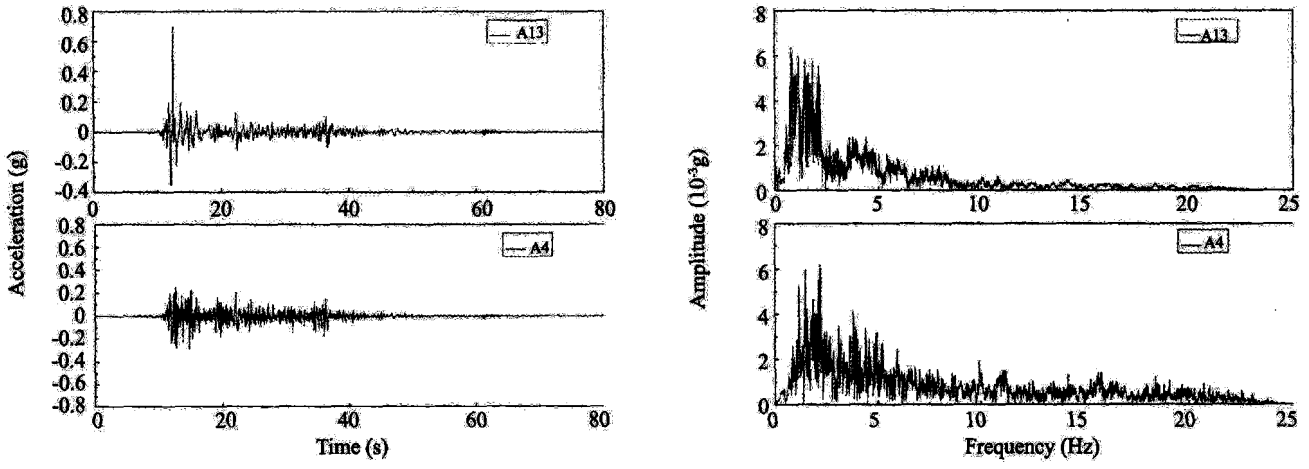

Fig. 8 Acceleration time histories (left) and corresponding Fourier spectra (right) of the ground in the free field in Event D

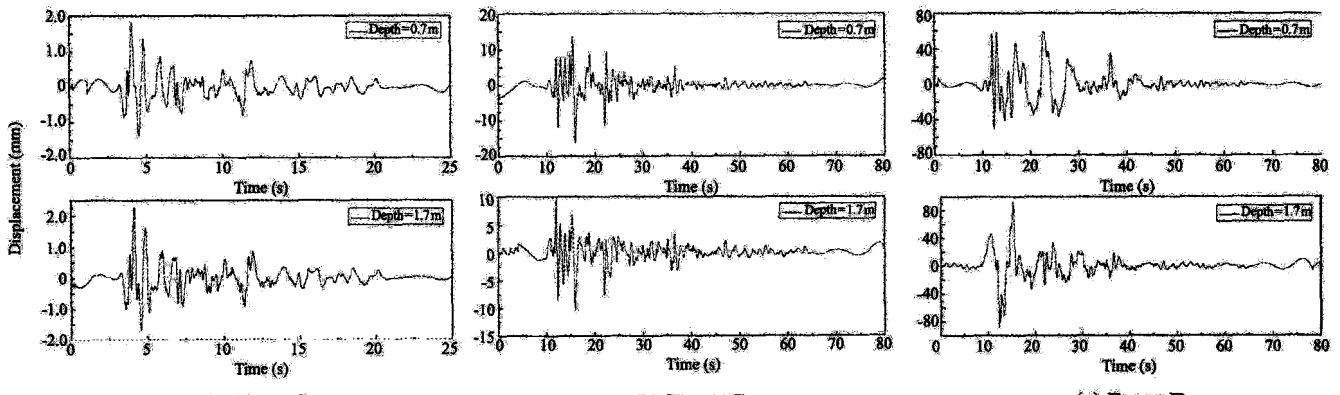

(a) Event B (b) Event C (c) Event D

Fig. 9 Displacement time histories of sand under three earthquake events

3.4 Acceleration response of pile and pier

Figures 10 through 12 indicate acceleration time histories and the corresponding Fourier spectra of the pile. Since the piles resisted the input acceleration at small magnitudes, remained linear in the incompletely liquefied ground, and the soil firmly restricted the piles, the acceleration response gradually attenuated from bottom to top in both Event B and Event C. The acceleration response of the pile can be attributed to the uniformity of the buildup and dissipation of EPP and the small EPP ratio in the sand layer in events B and C. However, the acceleration of the pile gradually increased from bottom to top in Event D, which might be related to factors such as the reduction of lateral support of the soil to the piles in fully liquefied sand, the decrease of the confinement effect of soil on the pile top, inertial forces of the superstructure, ground motion, and so on. In events B, C and D, the time when the acceleration reached its peak for the pile and at the top of the pier are almost consistent with the time when the input acceleration reached its peak, which

implied that the peak acceleration of the pile was mainly controlled by the input acceleration and seemed to be independent of the degree of liquefaction of the sand. Fourier components of the acceleration on the pile only continuously increased in the low frequency band from 0 Hz to 10 Hz from bottom to top; however it remained almost constant in the middle and high frequency band in events B, C and D. The acceleration time histories and the corresponding Fourier spectra of the pier are illustrated in Figs.13 to 15, and because of the combined

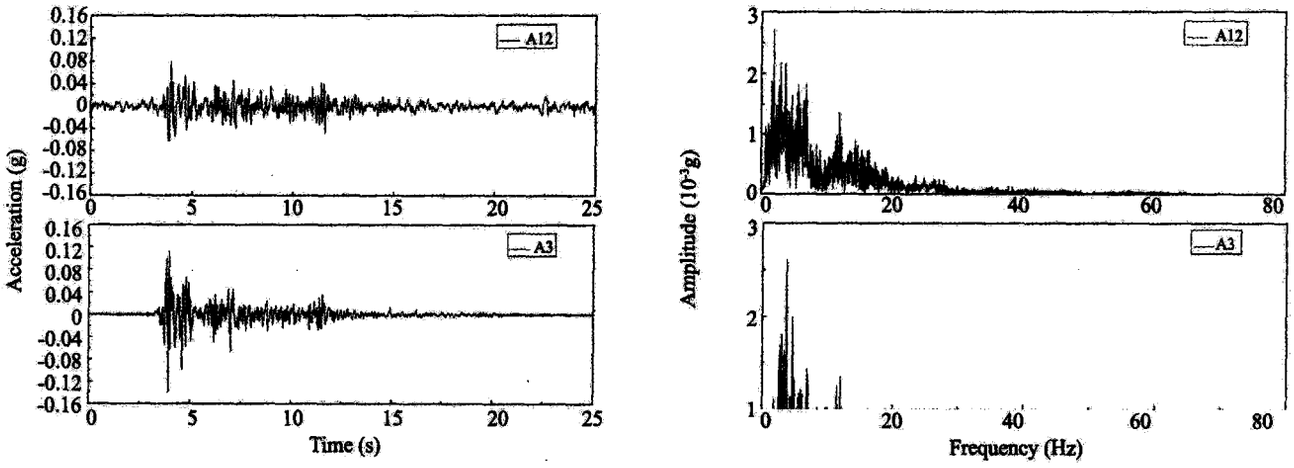

Fig. 10 Acceleration time histories and corresponding Fourier spectra of the pile in Event B

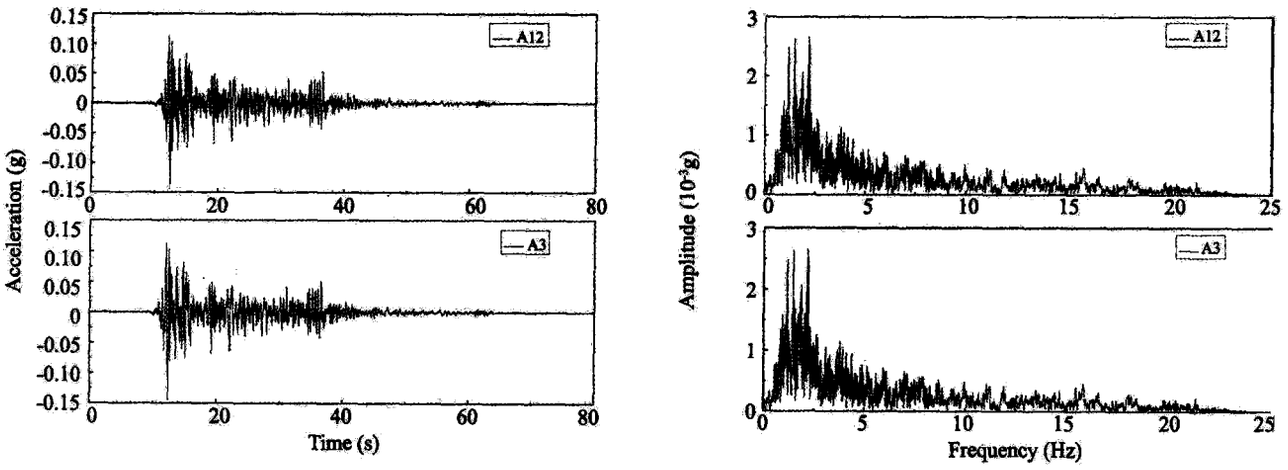

Fig. 11 Acceleration time histories (left) and corresponding Fourier spectra (right) of the pile in Event C

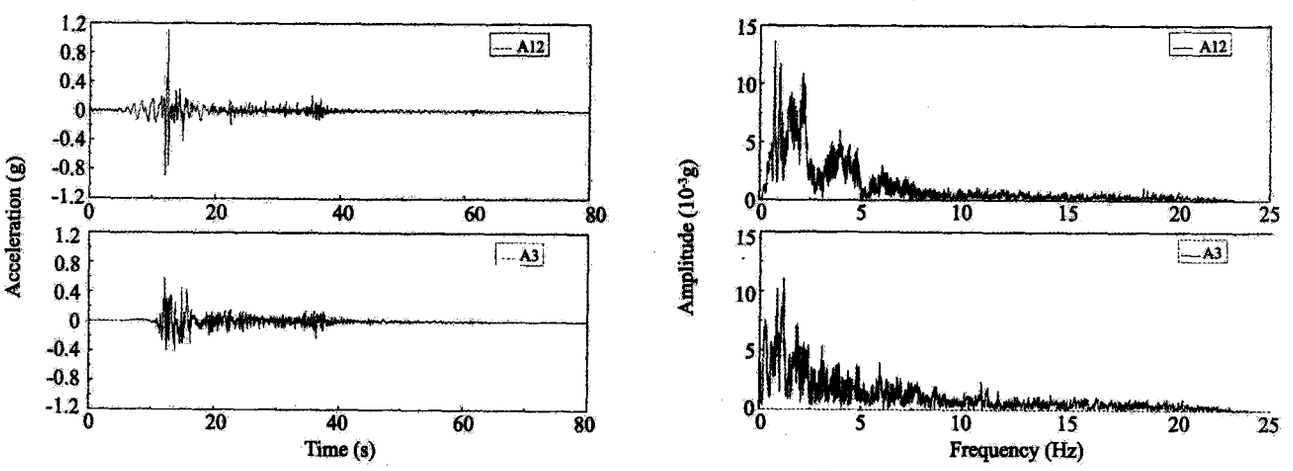

Fig. 12 Acceleration time histories (left) and corresponding Fourier spectra (right) of the pile in Event D

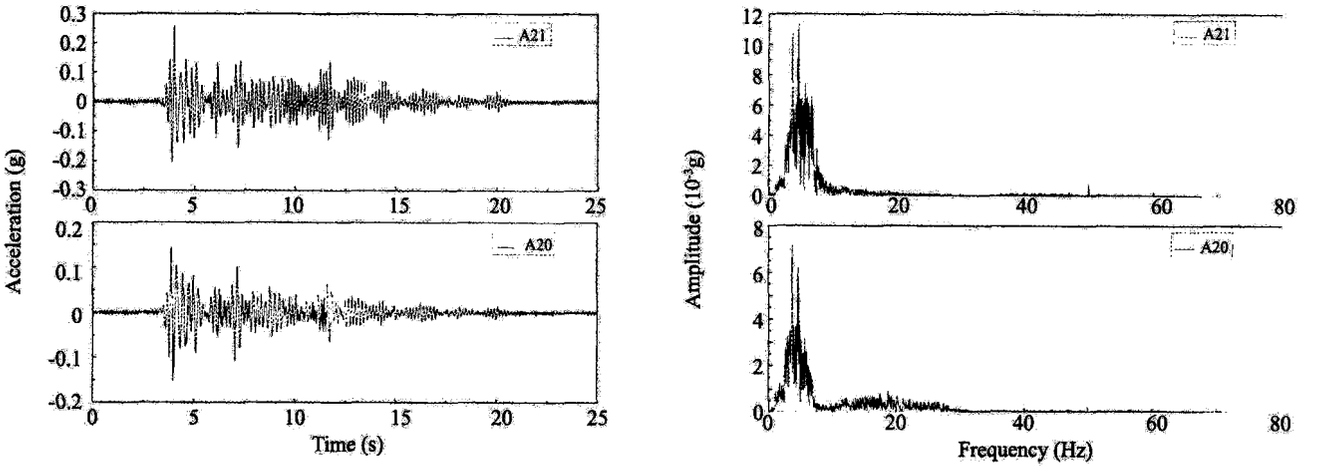

Fig. 13 Acceleration time histories and corresponding Fourier spectra of the pier in Event B

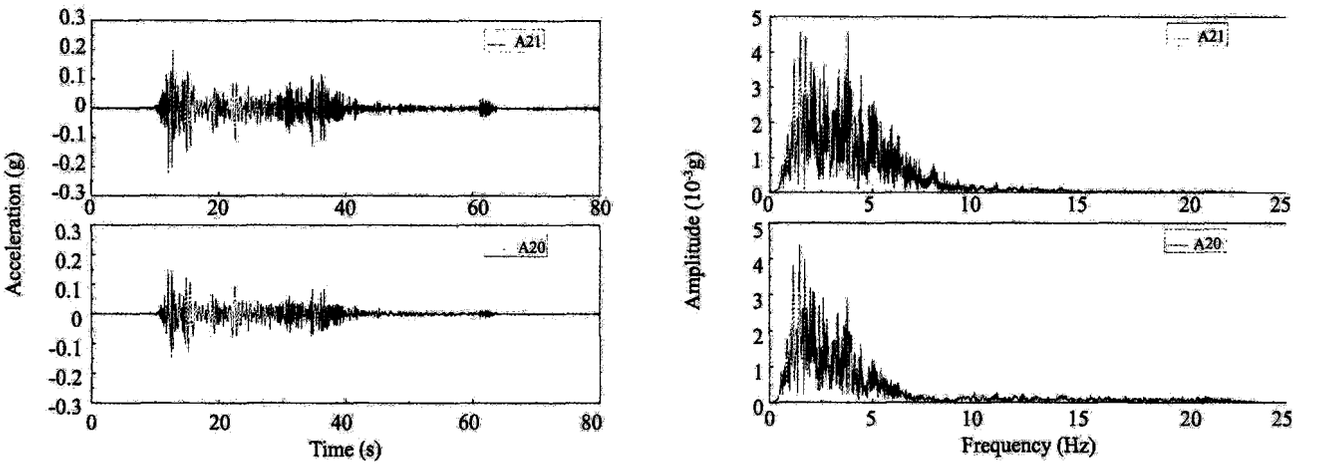

Fig. 14 Acceleration time histories (left) and corresponding Fourier spectra (right) of the pier in Event C

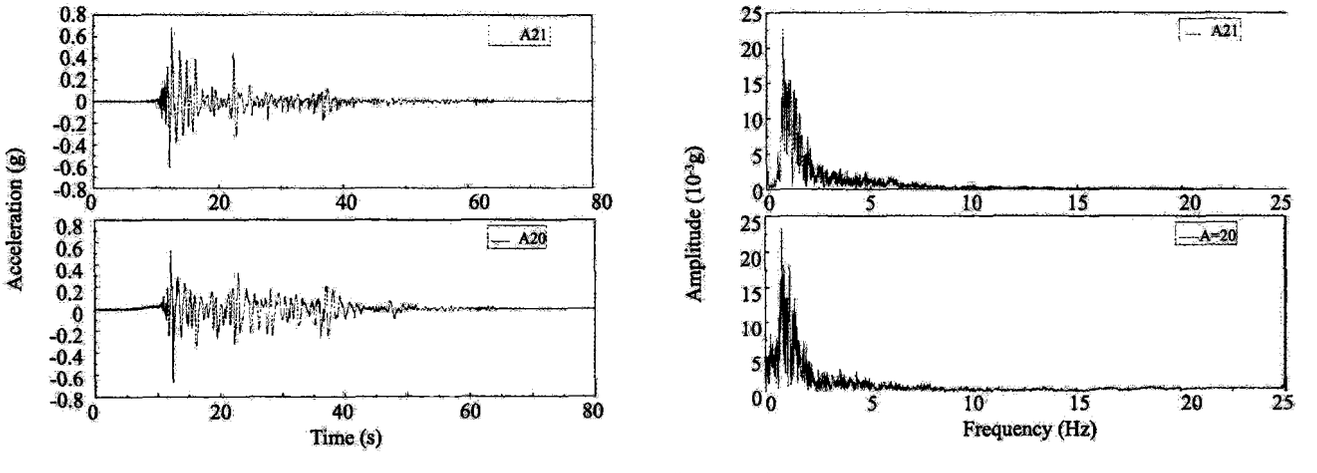

Fig. 15 Acceleration time histories (left) and corresponding Fourier spectra (right) of the pier in Event D

action of the inertial force of the superstructure, the rotation of the cap and soil movement, the acceleration of the pier was gradually magnified from bottom to top in events B, C and D. The acceleration response at the top of the pier was much larger in Event C than in Event B. However, in Event D, the acceleration amplification effect at the top of the pier slightly decreases, which is closely related to the soil liquefaction.

3.5 Moment of pile

The strains measured along the length of the pile had to be converted into curvature and moment data. From beam mechanics, it is known that strain, ε, is proportional to the curvature, k, and varies linearly with distance, h, from the neutral axis. A rearrangement of the strain-curvature relationship provides the following equation for the curvature:

$$k = \frac{\varepsilon}{h} \tag{1}$$

It should be recognized that the curvature depends solely on geometry and not material properties; therefore, Eq.1 is valid for linear as well as nonlinear elastic materials. When both sides of a symmetric pile are instrumented, the above equation becomes:

$$k = \frac{\varepsilon_t - \varepsilon_c}{2h} \tag{2}$$

where the subscripts, t and c, distinguish the strains measured on the tension and compression sides of the pile (with opposite signs), respectively. In the case of a round cross-section with gauges mounted to the exterior of the pile, the term $2h$ is equal to the diameter of the pile. After determining the curvature, the structural and material properties of the pile could then be used to determine the moment. The peak moment along the pile is presented in Fig.16 and the time histories of the moment on the pile are depicted in Fig.17 and in events B, C and D. Note that that the moment on the pile in the sand gradually increases from the bottom to the top in events B and C and the moment on the pile is larger in Event C than in Event B. The time when the peak moment occurs is consistent with the input acceleration and the acceleration at the top of the pier in Event B. The time when the maximum moment occurs agrees well with the peak sand displacement in Event C,

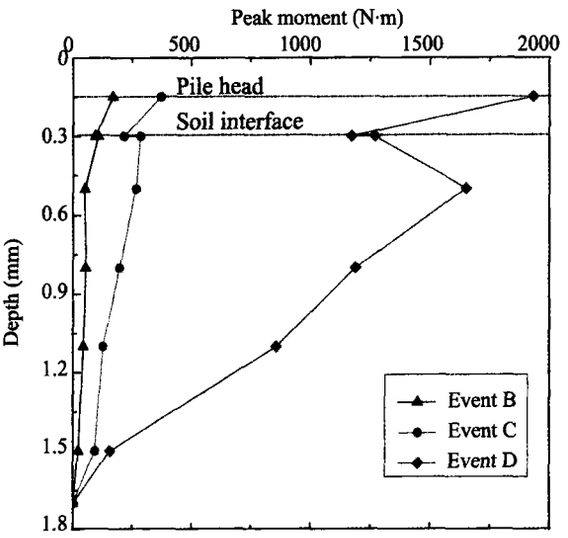

Fig. 16 Peak moment distribution of the pile in events B, C and D

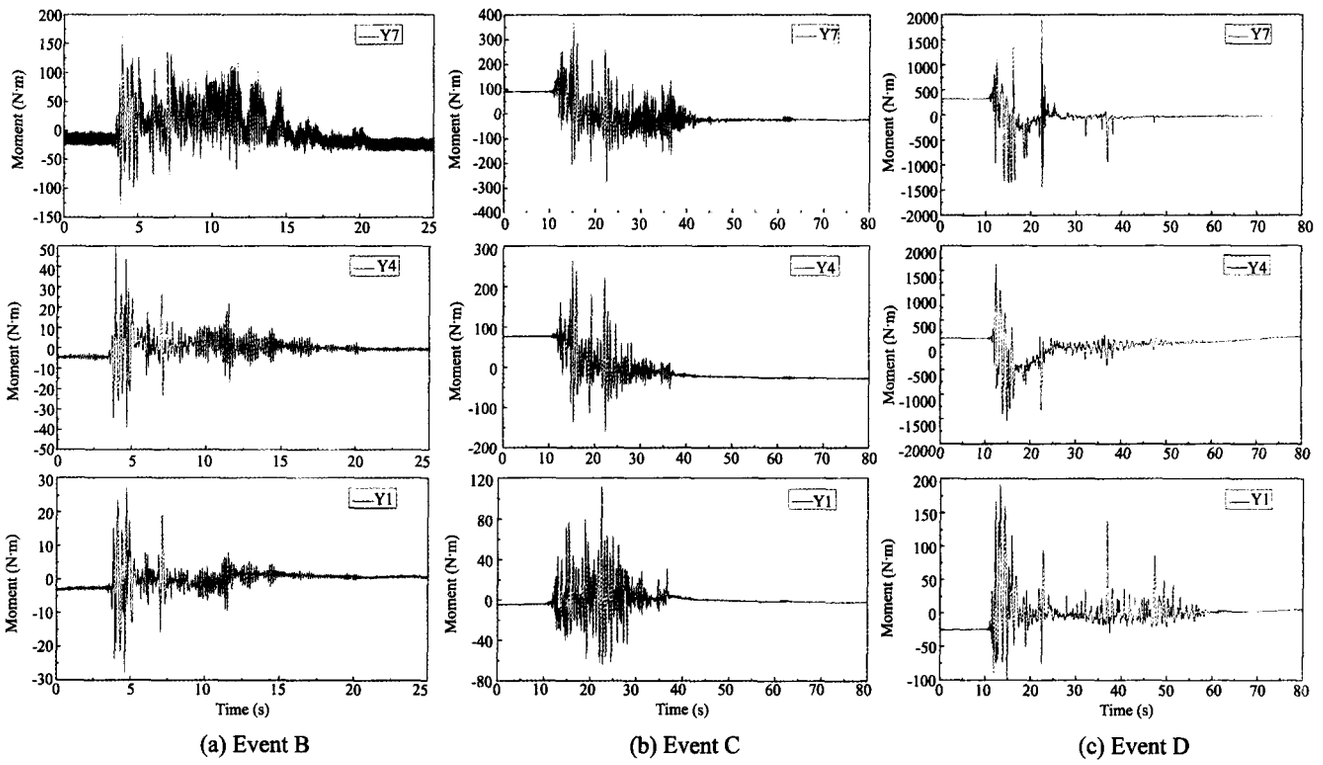

(a) Event B (b) Event C (c) Event D

Fig.17 Moment time histories at different locations of the pile in events B, C and D

and the same trend holds in Event D. The moment of the pile in the sand first gradually increases and then decreases from the bottom to the top in Event D. In all three earthquake events, though an abrupt change of the moment was found near the soil interface, the peak moment occurred at the pile heads. These facts indicate that the restriction from the upper clay layer and the cap on the pile heads are quite effective and the minimum moment occurred at the pile bottom because the pile tip was not fixed. Comparing the times when the sand displacement is reached and the input acceleration and moment of the pile reach their peaks, shows that the soil deformation had an obvious effect on the moment of the pile as soil liquefaction developed, and it is concluded that the amplitude of the input acceleration and the inertial effect of the superstructure might control the moment response of the pile when the EPP ratio is less than 0.3 in Event B. The soil deformation began to remarkably influence the moment on the pile when the EPP distinctly increased and the soil gradually displayed the liquefied characteristic in events C and D, especially in Event D. Therefore, special attention should be given to the contribution from the liquefied sand to the piles and the peak moment on the pile heads of low-cap pile groups in the seismic design of bridge piles in liquefiable ground.

4 Conclusions

The focus of this study is on the dynamic response of pile groups and bridge structures in liquefiable ground during an earthquake, using shake table testing. The major conclusions are as follows:

(1) The buildup of excess pore pressure (EPP) mainly depends on the soil depth and shaking duration. The EPP accumulates slowly during small-amplitude shaking and the accumulation mainly occurred during the strongest stage of shaking.

(2) The acceleration response of the sand layer is mainly related to the extent of the liquefaction. When the sand layer was not liquefied, the acceleration of the sand gradually decreased from the bottom to the top. However, as the sand began to liquefy, the acceleration of the sand layer gradually increased from the bottom to the top. In addition, there was a time delay when the input acceleration and sand displacement reached their peaks.

(3) With the development of soil liquefaction, the acceleration response of the pile changed from gradually decreasing to increasing in the vertical direction from the bottom to the top, the same as the acceleration response in the sand layer. The change in the Fourier components of the acceleration of the pile mainly occurred in the low-frequency band.

(4) Increase in the acceleration response of the pier was observed from bottom to top in all three earthquake events. The acceleration amplification effect at the top of the pier decreased due to soil liquefaction.

(5) Whether the sand liquefies or not, the peak moment on the pile occurs near the pile heads, and an abrupt change of the moment was observed near the soil interface in all three events. The effects of the sand liquefaction and pile heads should be accounted for in the seismic design of low-cap pile groups in bridges located on liquefiable ground.

Acknowledgement

The test was funded by Major Research Plan of National Natural Science Foundation of China Under Grant No. 90815009, National Natural Science Foundation of China Under Grant No. 50378031/ 50178027 and Western Transport Construction Technology Projects Under Grant No. 2009318000100, and was implemented in the State Key Laboratory for Disaster Reduction in Civil Engineering in China. This support is gratefully acknowledged. Also, the authors would like to thank the test personnel in the laboratory for their excellent support.

Reference

Abdoun T and Dobry R (2002), "Evaluation of Pile Foundation Response to Lateral Spreading," *Soil Dynamics and Earthquake Engineering*, **22**(9–11): 1051–1058.

Bhattacharya S (2003), "Pile Instability during Earthquake Liquefaction," Ph.D. Dissertation, University of Cambridge, Cambridge.

Boulanger RW, Curras CJ, Kutter BL, *et al* (1999), "Seismic Soil-pile-structure Interaction Experiments and Analyses," *Journal of Geotechnical and Geoenvironmental Engineering*, ASCE, **125**(9): 750–759.

Finn WDL and Fujita N (2002), "The Piles in Liquefiable Grounds: Seismic Analysis and Design Issues," *Soil Dynamics and Earthquake Engineering*, **22**: 731–742.

Fujii S, Cubrinovski M, Tokimatsu K, *et al* (1998), "Analyses of Damaged and Undamaged Pile Foundations in Liquefied Soils During the 1995 Kobe Earthquake," *Proc. 3rd Conf. Geotechnical Earthquake Engineering and Soil Dynamics*, ASCE, Seattle, pp.1187–1198.

Imamura S, Hagiwara T, Tsukamoto Y, *et al* (2004), "Response of Pile Groups Against Seismically Induced Lateral Flow in Centrifuge Model Tests," *Soils and Foundations*, **44**(3): 39–55.

Kagawa T, Minowa C, Mizuno H, *et al* (1994), "Shaking-Table Tests on Piles in Liquefying Sand," *Proc. 5th U.S. Natl. Conf. Earthquake Eng.*, Chicago, **V4**, pp. 107–116.

Li Yurun and Yuan Xiaoming (2004), "State-of-art of Study on Influences of Liquefaction-induced Soil Spreading over Pile Foundation Response," *World Earthquake Engineering*, **20**(2): 17–22. (in Chinese)

Ling Xianzhang, Wang Chen and Wang Cheng (2004), "Scale Modeling Method of Shaking Table Test of Dynamic Interaction of Pile-soil-bridge Structure in Ground of Soil Liquefaction," *Chinese Journal of Rock Mechanics and Engineering*, **23**(3): 450–456. (in Chinese)

Ling Xianzhang, Wang Lixia, Wang Dongsheng, *et al* (2005), "Study on Large-scale Shaking Table Proportional Model Test of the Dynamic Property of Foundation in Unfree Ground of Liquefaction," *China Journal of Highway and Transport*, **18**(2): 34–39. (in Chinese)

Ohtsuki A, Fukutake K and Sato M (1998), "Analytical and Centrifuge Studies of Pile Groups in Liquefiable Soil Before and After Site Remediation," *Earthquake Engineering and Structural Dynamics*, **27**(1): 1–14.

Shi Zhaoji and Wang Lanmin (1999), *Dynamic Property of Soil: Liquefaction Potential and Evaluation of Liquefaction Harmfulness*, Beijing: Seismic Press, 89–90. (in Chinese)

Wu Xiaoping, Sun Limin, Hu Shide, *et al* (2002), "Development of Laminar Shear Box Used in Shaking Table Test," *Journal of Tongji University*, **30**(7): 781–785. (in Chinese)